DEVELOPMENT OF CERAMIC WASTE FORMS FOR AN ADVANCED NUCLEAR FUEL CYCLE

A. L. Billings, K. S. Brinkman, K. M. Fox and J. C. Marra
Savannah River National Laboratory
Aiken, SC, USA

M. Tang and K. E. Sickafus
Los Alamos National Laboratory
Los Alamos, NM, USA

ABSTRACT

A series of ceramic waste forms were developed and characterized for the immobilization of a Cesium/Lanthanide (CS/LN) waste stream anticipated to result from nuclear fuel reprocessing. Simple raw materials, including Al_2O_3 and TiO_2 were combined with simulated waste components to produce multiphase ceramics containing hollandite-type phases, perovskites (particularly $BaTiO_3$), pyrochlores and other minor metal titanate phases. Three fabrication methodologies were used, including melting and crystallizing, pressing and sintering, and Spark Plasma Sintering (SPS), with the intent of studying phase evolution under various sintering conditions. X-Ray Diffraction (XRD) and Scanning Electron Microscopy coupled with Energy Dispersive Spectroscopy (SEM/EDS) results showed that the partitioning of the waste elements in the sintered materials was very similar, despite varying stoichiometry of the phases formed. Identification of excess Al_2O_3 via XRD and SEM/EDS in the first series of compositions led to a Phase II study, with significantly reduced Al_2O_3 concentrations and increased waste loadings. The Phase II compositions generally contained a reduced amount of unreacted Al_2O_3 as identified by XRD. Chemical composition measurements showed no significant issues with meeting the target compositions. However, volatilization of Cs and Mo was identified, particularly during melting, since sintering of the pressed pellets and SPS were performed at lower temperatures. Partitioning of some of the waste components was difficult to determine via XRD. SEM/EDS mapping showed that those elements, which were generally present in small concentrations, were well distributed throughout the waste forms.

INTRODUCTION

Efforts being conducted by the United States Department of Energy (DOE) under the Fuel Cycle Research and Development (FCR&D) program are aimed at demonstrating a proliferation-resistant, integrated nuclear fuel cycle. The envisioned fuel reprocessing technology would separate the fuel into several fractions, thus, partitioning the waste into groups with common chemistry. With these partitioned waste streams, it is possible to treat waste streams separately or combine waste streams for treatment when it is deemed appropriate. A trade study conducted in 2008 concluded that it was beneficial from a cost perspective to combine waste streams and treat them using existing waste form technologies.[1] A borosilicate glass was identified as the preferred waste form for the Cs/Sr (CS), lanthanide (LN) and transition metal fission product (TM) combined waste stream. Unfortunately, several fission products (e.g. noble metals and molybdenum) have limited solubility in borosilicate glasses. Therefore, the use of borosilicate glass may simplify waste form processing but result in significant increases in waste form volumes. This would defeat a major advanced fuel cycle reprocessing objective of minimizing high level waste form volumes. In this work, experimental work to develop crystalline ceramics to immobilize a combined CS and LN waste stream is discussed with a goal of obtaining high waste loadings and establishing baseline compositions for future CS/LN/TM combined waste stream work.

Titanate ceramics have been thoroughly studied for use in immobilizing nuclear wastes (e.g., the SYNROC family) due to their natural resistance to leaching in water.[2,3] Assemblages of several titanate phases have been successfully demonstrated to incorporate radioactive waste elements, and the multiphase nature of these materials allows them to accommodate variation in the waste composition.[4] While these materials are typically densified via hot isostatic pressing (HIP), recent work has shown that they can also be produced from a melt. For example, demonstrations have been completed using the Cold Crucible Induction Melter (CCIM) technology to produce several crystalline ceramic waste forms, including murataite-rich ceramics,[5] zirconolite/pyrochlore ceramics,[6] Synroc-C (zirconolite, hollandite, perovskite),[7] aluminotitanate ceramics, and zirconia.[8] This production route is advantageous since melters are already in use for commercial and defense high level waste (HLW) vitrification in several countries, and melter technology greatly reduces the potential for airborne contamination as compared to powder handling operations.

EXPERIMENTAL PROCEDURES

Waste Stream Composition and Chemical Additives

The CS/LN waste stream is a combination of the Cs/Sr separated stream and the Trivalent Actinide - Lanthanide Separation by Phosphorous reagent Extraction from Aqueous Komplexes (TALSPEAK) waste stream consisting of lanthanide fission products. In this testing, a projected composition for this combined stream was used (Table I).

Ceramic host systems for this study were selected based on the objectives of forming durable titanate and aluminate phases, using a minimum of additives to form the desired phases (i.e., achieving high waste loadings), and fabrication from a melt. Target compositions for the CS/LN waste form are given in Table II. The only additives used were Al_2O_3 and TiO_2, with targeted waste loadings of 50-60 wt %. The alkali and alkaline earth elements in the waste were anticipated to partition to aluminotitanate phases approximating hollandite or $(Ba,Cs,Rb)(Al,Ti)_2Ti_6O_{16}$. The lanthanides were anticipated to partition to aluminate perovskites $(LnAlO_3)$ and the strontium to a titanate perovskite $(SrTiO_3)$. Following characterization of the phase I samples, it was realized that titanate phases preferentially formed over aluminate phases (titanate phases thermodynamically more stable). Therefore, Phase II compositions were formulated with lower alumina concentrations (i.e. minimum alumina levels required to form the hollandite phase). The Phase II compositions are also given in Table II.

Table I. Composition of the CS/LN Waste Stream

Oxide	Wt %
Rb_2O	2.22
SrO	5.14
Y_2O_3	0.49
Cs_2O	15.08
BaO	11.55
La_2O_3	8.21
Ce_2O_3	15.28
Pr_2O_3	7.51
Nd_2O_3	27.11
Pm_2O_3	0.08
Sm_2O_3	5.58
Eu_2O_3	0.89
Gd_2O_3	0.84
Tb_2O_3	0.02

Table II. Target Compositions for the Phase I and Phase II CS/LN Ceramic Waste Forms.

Phase I			
Component	CS/LN-03	CS/LN-04	CS/LN-05
Waste	52	50	50
Al_2O_3	18	15	20
Phase II			
Component	CS/LN-06	CS/LN-08	CS/LN-09
Waste	50.0	55.0	60.0
Al_2O_3	4.0	7.3	8.0
TiO_2	46.0	37.7	32.0

Fabrication Methods

Simulated waste material and the ceramic forming additives were blended in the appropriate ratios via ball milling. Three different fabrication methods were used to densify the ceramic waste forms, including melting and crystallizing, cold pressing and sintering for extended periods, and rapid heating under pressure via spark plasma sintering. The intent was to provide insight into the phase assemblage that is formed at varying proximity to equilibrium conditions.

Samples of each of the ceramic materials were melted in an electric resistance heated furnace to simulate melter production. The blended and dried powders were placed into Pt/Rh alloy crucibles and melted at 1500°C for 1 hour. Power to the furnace was then turned off with the crucibles remaining inside to cool slowly (furnace cooling) to roughly approximate the slow cooling conditions experienced by a waste form poured from a melter into a canister. The temperature of the furnace fell below 200°C after 6.5 hours of cooling. The crucibles were removed from the furnace once cooled and photographed to document the degree of melting that occurred for each composition.

Sintering of pellets for longer periods was used to approximate equilibrium conditions and allow the more stable phases to form within each composition. The blended and dried powders were cold pressed into pellets using a steel die and uniaxial hydraulic press. Thermal analysis, conducted as a screening tool for crystallization and melting point determination, indicated that a majority of the compositions displayed initial melting point endotherms in the range of 1280-1300°C. The pellets were then sintered in an electric resistance heated furnace at 1200°C in air for 25 hours and furnace cooled.

Spark plasma sintering (SPS) is a powder densification process similar to hot pressing, except that heating occurs directly by passing a pulsed DC current through the die and powder rather than using resistive heating elements. This allows for very rapid heating of the powder and enhanced sintering due to high localized temperatures at particle interfaces, electric field assisted diffusion, and plastic deformation. Materials can typically be sintered via SPS at temperatures much lower than those of other sintering techniques and in much shorter times. SPS was explored for the ceramic waste forms to gauge the impacts of sintering at conditions far from equilibrium on the resulting phase assemblages. One sample (CS/LN-03) was sintered via SPS. Approximately 2 g of the sample powder was placed in a graphite die of approximately 20 mm diameter lined with graphite foil. The loaded die set was placed into the SPS chamber and a pressure of 3 MPa was applied. The chamber was evacuated and then backfilled with argon to 9.4×10^{-4} Torr. The sample was then heated from room temperature to 600°C at a rate of 150°C per minute using a DC pulse duration of 25 ms on and 5 ms off. The pressure was increased from 3 to 10 MPa during this time. The sample was held at 600°C for 15 seconds. Heating then continued at 100°C per minute to 1300°C, with the pressure being increased from 10 to 100 MPa during this time. The sample was held at 1300°C and 100 MPa for 15 minutes. The pressure was then relieved and the current was turned off to allow the sample to cool.

Sample Characterization

Representative samples of select compositions were characterized to confirm that the as-fabricated ceramics met the target compositions. A lithium-metaborate fusion was used to dissolve the samples. The resulting solutions were analyzed by Inductively Coupled Plasma – Atomic Emission Spectroscopy (ICP-AES). Two measurements were taken for each element of interest, and the average of these two measurements was reported as the measured value. Inductively Coupled Plasma – Mass Spectroscopy (ICP-MS) was used to measure the concentrations of Cs, Pd, Rh, and Ru. Only one measurement was performed for each of these elements.

Scanning Electron Microscopy (SEM) and Energy Dispersive Spectroscopy (EDS) analyses were performed on select samples. Specimens were cut, ground, and polished with alumina lapping films to produce a flat surface for imaging and analysis. All of the samples were final polished using 40 nm colloidal silica slurry to remove mechanical polishing damage. Secondary electron and backscattered electron imaging were used to identify grain size and morphology, as well as general homogeneity of the specimen. EDS elemental mapping was used to identify partitioning of the waste elements among the various phases.

Representative samples of each ceramic waste form were analyzed using X-ray diffraction (XRD) to assess phase development. Samples were ground prior to analysis. In some cases, the surfaces of unground samples were first analyzed to determine any differences between surface and bulk phase assemblage.

RESULTS AND DISCUSSION

Fabrication of the Ceramic Waste Forms

Photographs of the Phase I CS/LN waste forms fabricated from 1500°C melts are shown in Figure 1. Each of the three compositions appeared to have melted completely, with some void spaces after cooling and a mottled appearance that may be indicative of their multiphase composition.
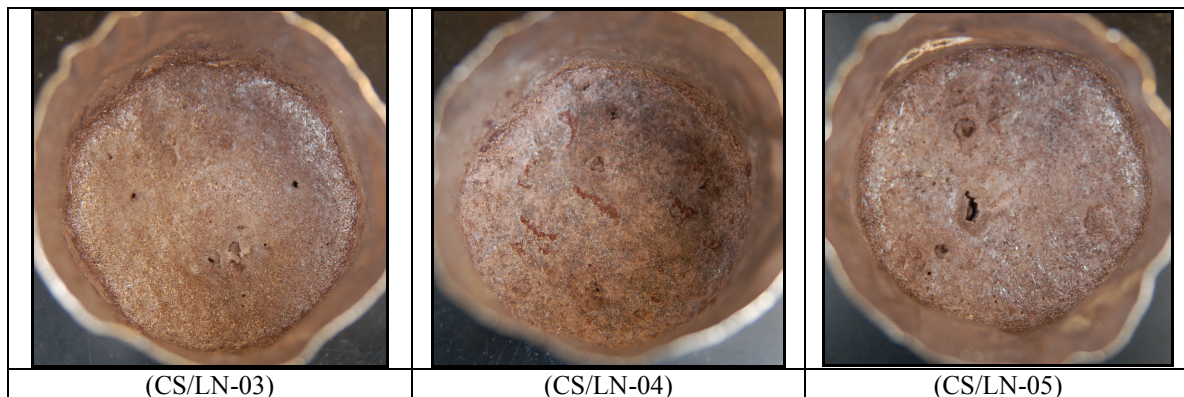

| (CS/LN-03) | (CS/LN-04) | (CS/LN-05) |

Figure1. Photographs of the Phase I CS/LN waste forms after melting and crystallizing.

Photographs of the Phase II CS/LN waste forms fabricated from 1500°C melts are shown in Figure 2. The CS/LN-06 and -08 compositions appeared to have melted completely. The CS/LN-09 composition, which has a higher concentration of waste oxides and Al_2O_3 in place of TiO_2, appears to have become too refractory to melt completely at 1500°C.

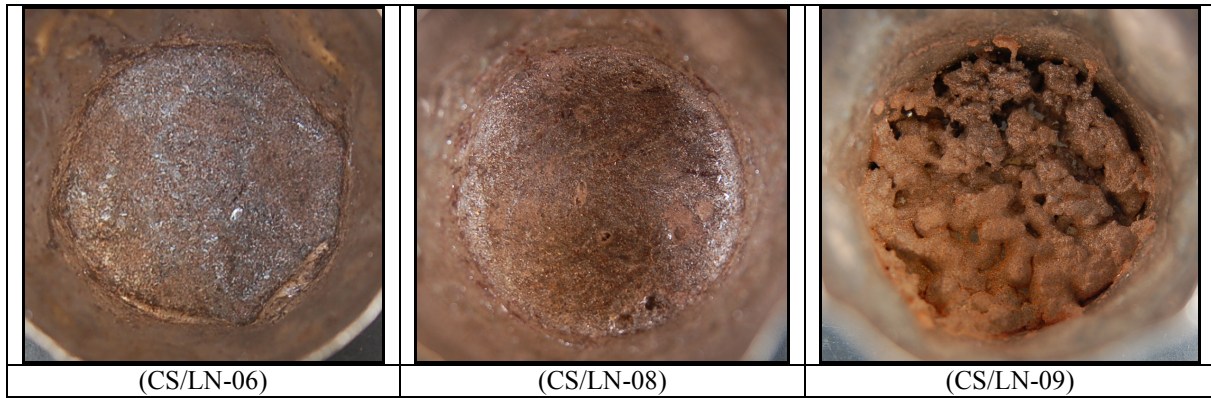| (CS/LN-06) | (CS/LN-08) | (CS/LN-09) |

Figure 2. Photographs of the Phase II CS/LN waste forms after melting and crystallizing.

Chemical Composition Measurements

The chemical compositions of CS/LN waste forms fabricated by melting and crystallizing were measured and compared to the target compositions. In general, most of the components were present at concentrations close to their targeted values. The Cs_2O concentrations were about 20-30% below their targeted values, which was likely due to volatilization during melting. There may have also been some volatilization of La_2O_3.

Microstructure and Elemental Analysis

Samples of compositions CS/LN-05 fabricated by melting and crystallizing and composition CS/LN-09 fabricated by pressing and sintering were analyzed using SEM/EDS. A backscattered electron micrograph of composition CS/LN-05 is shown in Figure 3a while a secondary electron micrograph of CS/LN-09 is shown in Figure 3b. The differences in contrast in Figure 3a indicated at least four crystalline phases were present in the CS/LN-05 sample prepared by melting and crystallizing, with varying grain sizes and morphology. Porosity is visible as the black area at the left of the micrograph. The more angular black areas may indicate grain pullout during polishing.
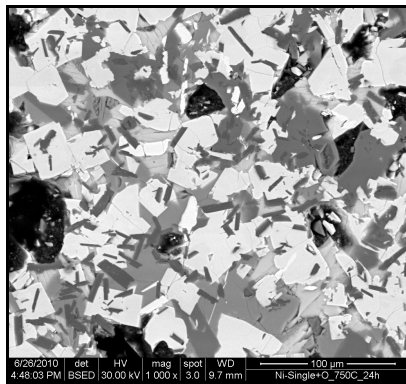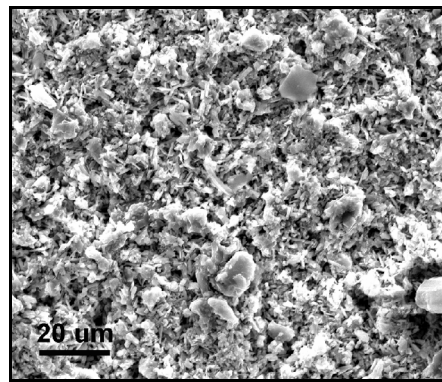
| (a) | (b) |

Figure 3. Electron micrographs of polished surfaces of (a) composition CS/LN-05 fabricated by melting and crystallizing (backscattered image) and (b) composition CS/LN-09 fabricated by pressing and sintering (secondary electron image).

The results of EDS elemental mapping for this sample are shown in Figure 4. Observations of these maps showed that:

- Unreacted Al_2O_3 was readily apparent as high aspect ration, or needle-like grains.
- Ba appeared to partition mainly to a titanate phase, but is present in all of the phases except for the unreacted Al_2O_3.
- Ce appeared to partition most strongly to a different titanate phase, with additional Ba and Nd.
- Cs and La appeared to partition to the same phase, although La is also distributed in other phases.
- Nd and Pr appeared to partition to the same phases.
- O is dispersed throughout the material as expected, although higher concentrations appeared with Al.
- Rb and Sr were distributed fairly uniformly, although some of the Sr appeared to partition to the phase containing Nd and Pr.

The secondary electron micrograph of composition CS/LN-09 (Figure 3b) was obtained from a rough cut surface of this sample since its low density made polishing difficult. This Phase II composition contained a lower concentration of Al_2O_3, and did not appear to contain the elongated grains of excess Al_2O_3 seen in the Phase I sample. The average grain size appeared to be smaller than that of the previous sample, with most grains measuring less than 10 μm in diameter. Porosity continued to be apparent. The secondary electron image did not allow for an estimate of the number of phases present based on z-contrast. However, the image suggested at least two phases based on the morphology of the grains: a phase with high aspect ratio platelet or needle-like grains, and a phase with larger diameter and smaller aspect ratio grains.

The results of EDS elemental mapping for the CS/LN-09 sample are shown in Figure 5. Observations of these maps showed that:

- There were still a small number of unreacted Al_2O_3 grains present, although they were not the high aspect ratio grains seen in the previous samples. The Al_2O_3 grains did not incorporate any of the other elements analyzed.
- Ba and Ti were distributed throughout the sample except for the Al_2O_3 grains, but were in the highest concentrations together.
- Ce was distributed throughout the sample, with a few grains of higher concentration. The results for Cs were similar, although the grains with higher Cs concentrations were different from those with higher Ce concentrations.
- La, Nd, Pr, and Sm, were fairly evenly distributed throughout the sample.
- Sr appeared evenly distributed among some of the phases and depleted in others.

The results of the EDS mapping were used to aid in the identification of the crystalline phase assemblages, along with the XRD data discussed in the following section.
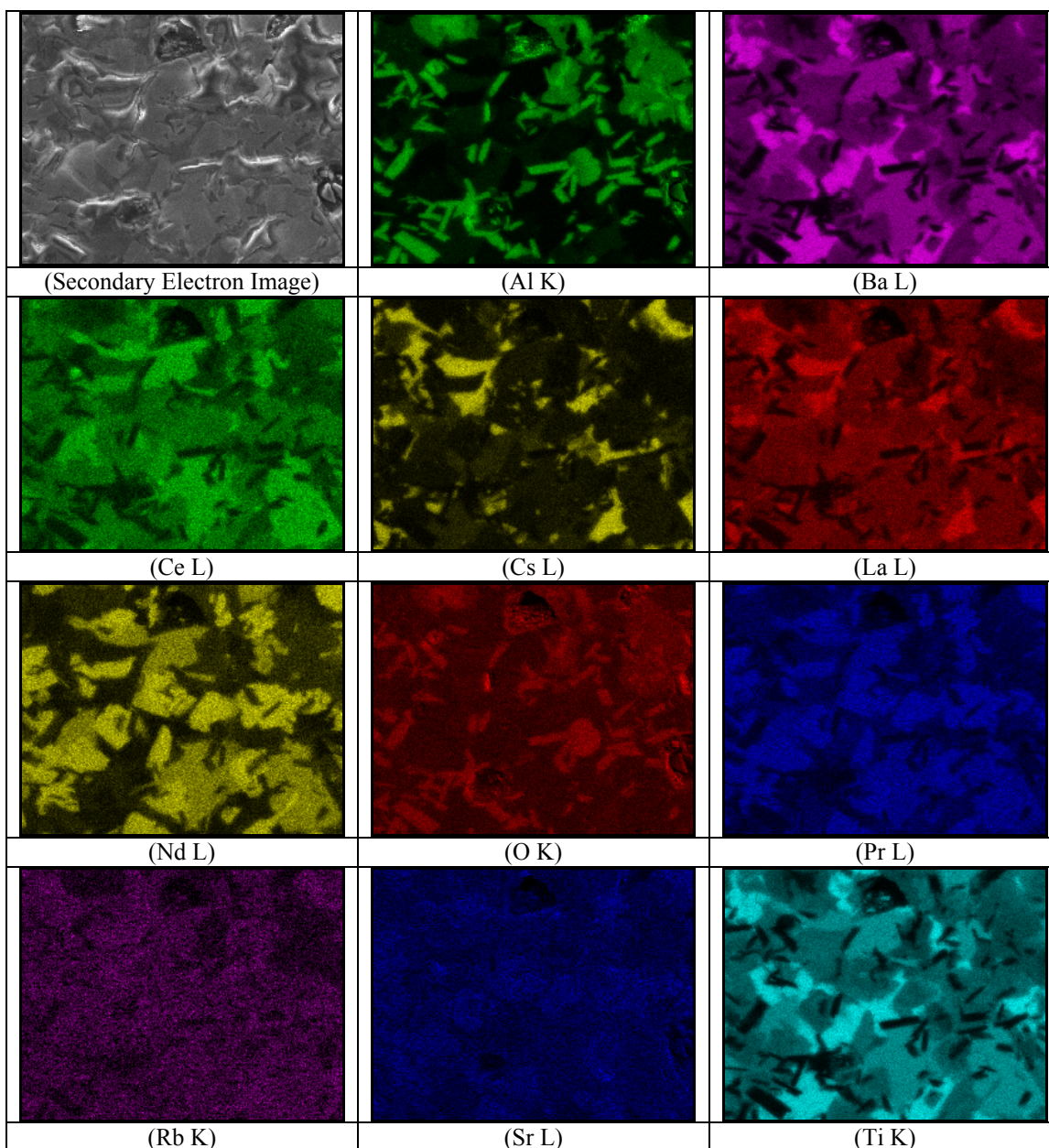
Figure 4. EDS mapping for select elements in composition CS/LN-05 fabricated by melting and crystallizing. The element and emission line are given for each image.

Phase Analysis

XRD data for the Phase I CS/LN compositions prepared via the three fabrication methods are summarized in Table III. XRD scans of the pellet surfaces and ground samples of the same material showed no texturing effects. The XRD data showed that some of the expected phases in the CS/LN system formed, while others did not. There was some dependence on the type of fabrication method used. The hollandite-type phases formed in each of the compositions as predicted. For the press and sinter method, $(Ba,Cs,Rb)Al_2Ti_5O_{14}$ was identified. The higher temperature processes produced $CsTiAlO_4$ and $(Ba,Cs)(Al_2Ti_6)O_{16}$ phases approximating hollandite. All of the methods produced the predicted $SrTiO_3$ perovskite phase, as well as $BaTiO_3$.
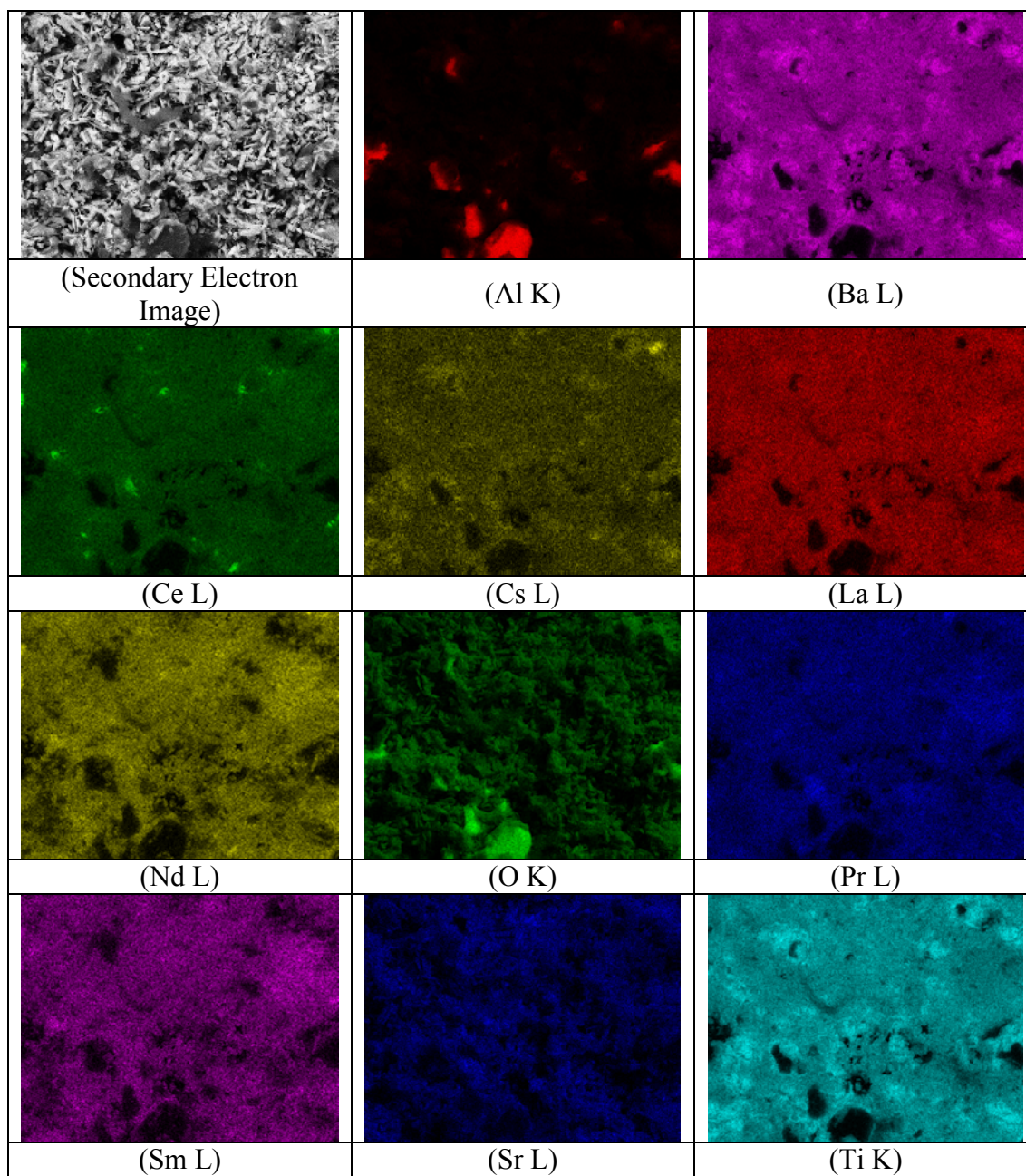
Figure 5. EDS mapping for select elements in composition CS/LN-09 fabricated by pressing and sintering. The element and emission line are given for each image.

The LnAlO$_3$ phases predicted to host the lanthanides for the CS/LN waste composition did not form. Instead, a Ba$_4$(Sr$_2$Sm$_8$)(TiO$_3$)$_{18}$ phase was detected in all of the compositions, as well as a Nd$_2$Ti$_2$O$_7$ pyrochlore phase potentially with all the fabrication methods except for the SPS sample. The Nd$_2$Ti$_2$O$_7$ pyrochlore phase in the samples produced from melts was difficult to positively identify by XRD but the SEM and EDS results served to confirm the presence of this phase (see Figure 4). A brief review of thermodynamic data for these phases shows that the lanthanide titanate phases should indeed be more stable than the lanthanide aluminate phases originally predicted to form. The most prevalent lanthanide in the CS/LN waste stream is Nd, and the free energy of formation of NdAlO$_3$ is approximately -41 kJ/mol,[9] as compared to approximately -120 kJ/mol for Nd$_2$Ti$_2$O$_7$.[10] Although the

conditions used to fabricate these compositions were likely not at equilibrium, the lower free energy of formation of $Nd_2Ti_2O_7$ is in agreement with the XRD results.

Partitioning of the waste components Ce, La, and Pr was not clear from the XRD data. Based on the EDS results (and XRD results for the Phase II compositions discussed below), it was likely that these components were present as substitutional cations in the perovskite phase. Corundum (Al_2O_3) was identified in all of the samples, indicating that an excess of Al_2O_3 was added to the compositions and remained unreacted after melting or sintering. This finding led to the reduced Al_2O_3 concentrations targeted in the Phase II compositions (see Table II).

XRD data for the Phase II CS/LN compositions prepared via two of the fabrication methods (the Phase II compositions were not sintered by SPS) are summarized in Table IV. For most of the compositions fabricated by pressing and sintering, the predicted hollandite-type phases were formed, as well as Ba perovskite and Nd pyrochlore phases. CS/LN-06, which had the lowest target Al_2O_3 concentration, had no unreacted Al_2O_3 detectable by XRD. Titanate phases differing from a typical hollandite stoichiometry formed in the CS/LN-08 and -09 compositions, but may have similar structures.

For most of the Phase II CS/LN compositions fabricated by melting and crystallizing, hollandite-type and pyrochlore phases again formed. No perovskites or unreacted Al_2O_3 were detected in these samples via XRD. However, the EDS data (Figure 5) showed unreacted Al_2O_3 in composition CS/LN-09. Cs partitioned to an aluminotitanate phase in most of these samples. The alkaline earths, transition metals and some of the lanthanides also partitioned to titanate phases. The predicted $LnAlO_3$-type phases did not form using either fabrication method, which again may be due to a larger free energy of formation of these phases as compared to the titanates.

Partitioning of the Ce, Cs, La, and Pr in the Phase II CS/LN compositions was unclear from the XRD data. The Ce, La, and Pr may have partitioned to the perovskite phase as identified for some of the Phase I compositions. The EDS data showed these elements to be fairly well distributed throughout the material (see Figure 5).

Table III. Summary of XRD Data for Phase I CS/LN Waste Forms Prepared by Three Methods

Phases	Press and Sinter			Melt and Crystallize			SPS
	CS/LN-03	CS/LN-04	CS/LN-05	CS/LN-03	CS/LN-04	CS/LN-05	CS/LN-03
$BaTiO_3/SrTiO_3$ perovskite	X	X	X	X	X	X	X
$CsTiAlO_4$ hollandite type				X	X	X	X
$(Ba,Cs)(Al_2Ti_6)O_{16}$ hollandite type							X
$(Ba,Cs,Rb)Al_2Ti_5O_{14}$ hollandite	X	X	X				
$Ba_4(Sr_2Sm_8)(TiO_3)_{18}$	X	X	X	X	X	X	X
$Nd_2Ti_2O_7$ pyrochlore	X	X	X	?	?	X (SEM/EDS)	
Unreacted Al_2O_3	X	X	X	X	X	X	X

Table IV. Summary of XRD Data for Phase II CS/LN Waste Forms Prepared by Two Methods

Phases	Press and Sinter			Melt and Crystallize		
	CS/LN-06	CS/LN-08	CS/LN-09	CS/LN-06	CS/LN-08	CS/LN-09
$Sr_{0.34}Nd_{2.44}Ti_4O_{12}$				X	X	
$BaNd_2Ti_4O_{12}$			X	X		X
$BaAlTi_5O_{14}$ Hollandite	X	X		X	X	
$Nd_2Ti_2O_7$ Pyrochlore	X	X	X		X	X
$Cs_2Ti_2Al_2O_8$					X	X
$BaTiO_3$ perovskite	X	X	X			
Unreacted Al_2O_3		X	X			X (SEM/EDS)
$Ba_4(Sr_2Sm_8)(TiO_3)_{18}$		X	X			

CONCLUSIONS

A series of ceramic waste form compositions for the immobilization of CS/LN waste streams anticipated to result from nuclear fuel reprocessing were developed. Three fabrication methodologies were used, including melting and crystallizing, pressing and sintering, and SPS, with the intent of studying phase evolution under various sintering conditions. XRD and SEM/EDS results showed that the partitioning of the waste elements in the materials was very similar, despite varying stoichiometry of the phases formed. The Phase II compositions generally contained a reduced amount of unreacted Al_2O_3 as identified by XRD. They also had phase assemblages that were closer to the initial targets. Chemical composition measurements showed no significant issues with meeting the target compositions. However, volatilization of Cs and La was identified, particularly during melting, since sintering of the pressed pellets and SPS were preformed at lower temperatures. Partitioning of some of the waste components was difficult to determine via XRD. EDS mapping showed that these elements, which were generally those present in smaller concentrations, were well distributed throughout the waste forms.

REFERENCES
[1] D. Gombert, S. Piet, T. Trickel, J. Carter, J. D. Vienna and W. Ebert, "Combined Waste Form Cost Trade Study," *U.S. Department of Energy Report GNEP-SYSA-PMO-MI-DV-2009-000003,* Idaho National Laboratory, (2008).

[2] A. E.Ringwood, E. S. Kesson, N. G. Ware, W. Hibberson and A. Major, "Geological Immobilisation of Nuclear Reactor Wastes," *Nature,* **278** 219 (1979).

[3] A. E. Ringwood, E. S. Kesson, K. D. Reeve, D. M. Levins and E. J. Ramm, "Synroc," pp. 233-334 in *Radioactive Waste Forms for the Future,* W. Lutze and R. C. Ewing, eds. Elsevier, North-Holland, Amsterdam, Netherlands (1988).

[4] D. S. Perera, B. D. Begg, E. R. Vance and M. W. A. Stewart, "Application of Crystal Chemistry in the Development of Radioactive Wasteforms," *Advances in Technology of Materials and Materials Processing,* **6** [2] 214-217 (2004).

[5] S. V. Stefanovsky, A. G. Ptashkin, O. A. Knyazev, S. A. Dmitriev, S. V. Yudintsev and B. S. Nikonov, "Inductive Cold Crucible Melting of Actinide-bearing Murataite-based Ceramics," *Journal of Alloys and Compounds,* **444-445** 438-442 (2007).

[6] A. V. Demine, N. V. Krylova, P. P. Polyektov, I. N. Shestoperov, T. V. Smelova, V. F. Gorn and G. M. Medvedev, "High Level Waste Solidification Using a Cold Crucible Induction Melter"; pp. 27-34 in Mater. Res. Soc. Symp. Proc., Vol. 663, *Scientific Basis for Nuclear Waste Management XXIV.* Edited by K. P. Hart and G. R. Lumpkin. Warrendale, PA, 2001.

[7] T. Advocat, G. Leturcq, J. Lacombe, G. Berger, R. A. Day, K. Hart, E. Vernaz and A. Bonnetier, "Alteration of Cold Crucible Melter Titanate-based Ceramics: Comparison with Hot-Pressed Titanate-based Ceramic"; pp. 355-362 in Mater. Res. Soc. Symp. Proc., Vol. 465, *Scientific Basis for Nuclear Waste Management XX.* Edited by W. J. Gray and I. R. Triay. Pittsburgh, PA, 1997.

[8] G. Leturcq, T. Advocat, K. Hart, G. Berger, J. Lacombe and A. Bonnetier, "Solubility Study of Ti Zr-based Ceramics Designed to Immobilize Long-lived Radionuclides," *American Mineralogist,* **86** [7-8] 871-880 (2001).

[9] J. E. Saal, D. Shin, A. J. Stevenson, G. L. Messing and Z.-K. Liu, "First-Principles Calculations and Thermodynamic Modeling of the Al_2O_3-Nd_2O_3 System," *Journal of the American Ceramic Society,* **91** [10] 3355-3361 (2008).

[10] K. B. Helean, S. V. Ushakov, C. E. Brown, A. Navrotsky, J. Lian, R. C. Ewing, J. M. Farmer and L. A. Boatner, "Formation Enthalpies of Rare Earth Titanate Pyrochlores," *Journal of Solid State Chemistry,* **177** [6] 1858-1866 (2004).